

# Spectral Analysis of Light Rayleigh Scattered on Macromolecules Reoriented by a Laser Beam

M. DĘBSKA-KOTŁOWSKA AND A. MIRANOWICZ

*Nonlinear Optics Division, Institute of Physics, Adam Mickiewicz University, 60-780 Poznań, Poland*

Received December 1, 1994; accepted April 27, 1995

IN MEMORY OF PROFESSOR STANISŁAW KIELICH (1925–1993)

The spectral analysis of light Rayleigh scattered by monodisperse solutions of rigid, anisotropic macromolecules in the reorienting electric field of a laser beam is presented. Formulas for the spectral lineshapes of the polarized and depolarized intensities of scattered light are derived, taking into account the rotational and translational diffusion of the macromolecules in the laser field. From our numerical computations, the influence of the shape and size of the macromolecules and the influence of the reorientation parameter of their polarizability ellipsoid on the lineshapes of the respective scattered light components at a low degree of reorientation in the laser field are determined. © 1995 Academic Press, Inc.

## 1. INTRODUCTION

Optical macromolecular light scattering investigations have been greatly developed due to the progress in laser techniques (1–4), leading to the determination of the dynamics of the scatterers (5–8).

Here, we report results for the polarized and depolarized intensity components of spectral lines Rayleigh scattered by monodisperse solutions of rigid, anisotropic macromolecules in the Rayleigh–Debye–Gans (RDG) approximation (see Ref. 9), reoriented by the strong electric field of laser light polarized vertical to the plane of observation.

Formulas for the scattered components are derived by us for the generalized Smoluchowski–Debye model of molecular diffusion in liquids (see Refs. 10, 11). We analyze the case of bidiametric molecules, also considering other kinds of anisotropy. In particular, we consider the influence of macromolecular rotational and translational diffusion in an external electric reorienting field on the lineshapes of the scattered light components. We assume statistical independence of rotational and translational diffusion.

We shall restrict our considerations to the case of a low degree of reorientation of macromolecules in the

electric field of a laser beam. Our formulas describe the spectral line intensities for the scattered light components. Next, on the basis of numerical computations, we discuss the shape of the lines as a function of the size of the macromolecules, compared with the incident probe light wavelength  $\lambda$ , the shape of the macromolecules (rodlike or disclike), and the value of the reorientation parameter of their optical polarizability ellipsoid.

## 2. THEORY

We consider monodisperse, dilute solutions of rigid anisotropic macromolecules, not absorbing energy, and having the shape of a rod or disc with rotational ellipsoid symmetry. We assume the symmetry axis of their optical properties to coincide with their geometrical axis. Moreover, the solutions fulfill the conditions of the RDG approximation (9), i.e.,

$$2kL^w |n - 1| \ll 1,$$

where  $k = 2\pi/\lambda$  ( $\lambda$  is the wavelength of the incident probe beam, and  $L^w$  is the length of the rodlike macromolecule or the diameter of the disclike macromolecule).

We assume that the weak probe beam is incident along the laboratory  $Y$ -axis and that observation takes place in the direction of the  $X$ -axis. Figure 1 visualizes the various possible polarization directions of the incident and scattered waves. We assume the system to be acted on simultaneously by the electric field of a strong laser beam of intensity  $I_L^v$  polarized vertically.

We express the heterodyne autocorrelation function of the electric field amplitudes of the scattered light in the form of the second-rank Cartesian tensor  $I_{ij}^v(q', t)$  (12, 13) of the light intensity scattered by the macromolecular solution in the presence of the external electric field of a vertically polarized strong laser beam (superscript  $v$ ).

Applying the method of irreducible spherical tensors (13–

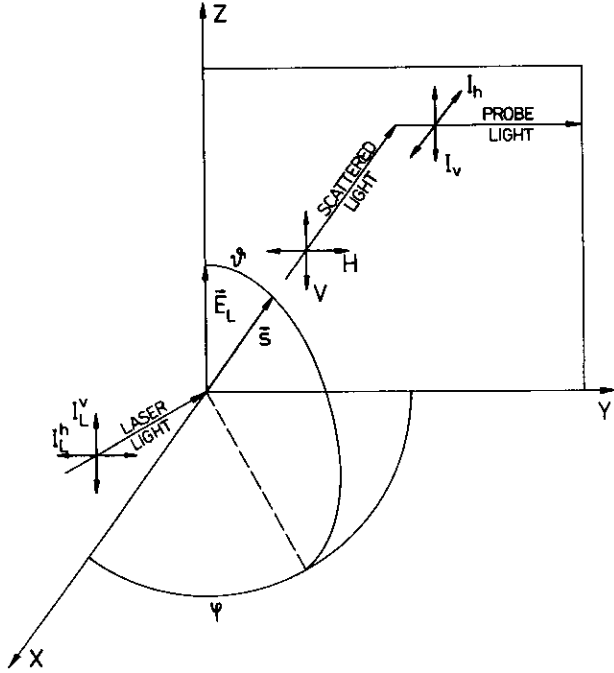


FIG. 1. Geometry of observation of light scattering. The probe light beam at frequency  $\omega$  is incident along the  $Y$ -axis of the laboratory coordinates. The indices  $v$  and  $h$  denote, respectively, the vertical and horizontal polarizations of the incident probe light. The observation is performed along the  $X$ -axis, with  $V$  and  $H$  denoting the vertical and horizontal components of the scattered light. The angle  $\vartheta$  lies between  $Z$  and the symmetry axis  $s$  of the macromolecule, and  $\varphi$  is the azimuth of  $s$ . The electric field  $E_L$  of the strong laser beam (with intensity  $I_L^v$  and frequency  $\omega_L$ ), which reorients the macromolecules, is polarized vertically along the  $Z$ -axis and propagates in the  $XY$ -plane.

16), we express the tensor  $I_{ij}^v(q', t)$  in laboratory coordinates  $X$ ,  $Y$ , and  $Z$  for a moment of time  $t$  as (8)

$$\begin{aligned}
 I_{ij}^v(q', t) = & A' \exp(-q'^2 D_T t) \sum_{n'} \sum_I \sum_J \sum_M \sum_N (-1)^M (-i)^{n'} \\
 & \times \frac{2N+1}{2I+1} \sqrt{2n'+1} C_I(I_L^v) C_{0M}^{JN}(t, I_L^v) \\
 & \times \left\{ \frac{i^J}{\sqrt{2J+1}} U_{00}^{ik} Y_{J,-M}^*(\Omega_{q'}) d_J(x) \right. \\
 & + \sqrt{2} \kappa_\omega \sum_m \sum_n \sum_{N_1} \frac{i^n}{\sqrt{2n+1}} U_{2N_1}^{ik} Y_{nm}^*(\Omega_{q'}) \\
 & \times \left[ \begin{matrix} J & 2 & n \\ 0 & 0 & 0 \end{matrix} \right] \left[ \begin{matrix} J & 2 & n \\ M & N_1 & -m \end{matrix} \right] b_n(x) \left. \right\} \\
 & \times \left\{ U_{00}^{j'k'} Y_{n',-M}(\Omega_{q'}) \left[ \begin{matrix} n' & N & I \\ 0 & 0 & 0 \end{matrix} \right] \right. \\
 & \times \left. \left[ \begin{matrix} n' & N & I \\ -M & M & 0 \end{matrix} \right] d_{n'}(x) \right\}
 \end{aligned}$$

$$\begin{aligned}
 & + \sqrt{2} \kappa_\omega \sum_{m'} \sum_G \sum_{N_2} U_{2N_2}^{j'k'} Y_{n'm'}(\Omega_{q'}) \\
 & \times \left[ \begin{matrix} n' & 2 & G \\ 0 & 0 & 0 \end{matrix} \right] \left[ \begin{matrix} n' & 2 & G \\ m' & N_2 & -M \end{matrix} \right] \\
 & \times \left. \left[ \begin{matrix} G & N & I \\ 0 & 0 & 0 \end{matrix} \right] \left[ \begin{matrix} G & N & I \\ -M & M & 0 \end{matrix} \right] b_{n'}(x) \right\} I_{kl}^0(t),
 \end{aligned} \tag{1}$$

where  $D_T$  is the translational diffusion constant of the macromolecule;  $U_{00}^{ik}, U_{00}^{j'k'}, \dots$  are the transformation coefficients between the spherical and Cartesian tensor components (Table 1);  $\left[ \begin{matrix} n' & N & I \\ 0 & 0 & 0 \end{matrix} \right], \left[ \begin{matrix} n' & N & I \\ -M & M & 0 \end{matrix} \right], \dots$  represent the Clebsch-Gordan coefficients;  $Y_{j,-M}^*(\Omega_{q'}), Y_{n',-M}(\Omega_{q'}), \dots$  are spherical harmonics dependent on the set of angles  $\Omega_{q'}$  determining the position of the scattering vector  $\mathbf{q}'$  ( $\mathbf{q}' = \mathbf{k}_0 - \mathbf{k}$ , where  $\mathbf{k}_0$  is the wave vector of the incident probe light and  $\mathbf{k}$  that of the scattered wave). The shape functions  $d_J(x), b_n(x), \dots$  for (i) rodlike macromolecules (prolate cylinders of height  $l$  much greater than their diameter  $2a_D$ , i.e.,  $l \gg 2a_D$ ) are (17)

$$\begin{aligned}
 d_J^R(x) &= \frac{1}{x} \int_0^x j_J(x') dx', \\
 b_n^R(x) &\equiv b_{n'0}^R(x) = d_n^R(x),
 \end{aligned} \tag{1a}$$

where  $x = \frac{1}{2} q' l$ , whereas for (ii) disclike macromolecules (oblate cylinders with  $l \ll 2a_D$ ) we have

TABLE 1  
Values of the Transformation Coefficients  $U_{LN_1}^{ik}$

$ik$	$LN_1$					
	00	20	22	2-2	21	2-1
xx	$\frac{1}{\sqrt{3}}$	$-\frac{1}{\sqrt{6}}$	$\frac{1}{2}$	$\frac{1}{2}$	0	0
yy	$\frac{1}{\sqrt{3}}$	$-\frac{1}{\sqrt{6}}$	$-\frac{1}{2}$	$-\frac{1}{2}$	0	0
zz	$\frac{1}{\sqrt{3}}$	$\frac{2}{\sqrt{6}}$	0	0	0	0
xy	0	0	$-\frac{i}{2}$	$\frac{i}{2}$	0	0
yz	0	0	0	0	$\frac{i}{2}$	$\frac{i}{2}$
zx	0	0	0	0	$-\frac{1}{2}$	$\frac{1}{2}$

$$d_J^D(x) = (-1)^{J/2} \frac{(J-1)!!}{J!} \frac{2}{x^2} \int_0^x j_J(x') dx',$$

$$b_{n'}^D(x) \equiv b_{n'0}^D(x) = -\frac{1}{2} d_{n'}^D(x), \quad [1b]$$

where  $x = q'a_D$ , and  $j_J(x')$  is a spherical Bessel function of order  $J$  (Eqs. [1a] and [1b] hold for even  $J$ ,  $n'$  only). The function  $A'$  in Eq. [1] is given by (8)

$$A' = 96\pi^3 a_\omega^2 \rho' \left(\frac{\omega}{c}\right)^4, \quad [1c]$$

where  $\rho'$  is the density of the macromolecules in the solution,  $\omega$  is the frequency of the incident probe light wave;  $c$  is the velocity of light; and the quantity

$$a_\omega = \frac{1}{3}(a_3^\omega + 2a_1^\omega) \quad [1d]$$

is the mean optical polarizability of the macromolecule ( $a_3^\omega$  and  $a_1^\omega$  are optical polarizabilities of the macromolecule along its axis of symmetry  $s$  and along the symmetry axis perpendicular thereto). Other quantities occurring in Eq. [1] are defined as

$$\kappa_\omega = \frac{a_3^\omega - a_1^\omega}{2a_1^\omega + a_3^\omega}, \quad [1e]$$

the optical anisotropy of the macromolecule, and

$$I_{ki}^0(t) = \frac{1}{2} E_{ok}(t) E_{oi}^*(0), \quad [1f]$$

the intensity tensor of the probe light incident on the scattering medium at  $t$ . The coefficients  $C_{0M}^{JN}(t, I_L^v)$  occurring in Eq. [1] are those of Debye rotational diffusion (6, 18). They intervene in the expansion of  $f(\Omega|\Omega_i, t, I_L^v)$  in a series of Wigner functions, determining the conditional probability density distribution of reorientation  $\Omega_i$  of the  $\mathbf{E}_L$  (directed along the  $Z$ -axis as depicted in Fig. 1) of the strong laser beam polarized vertically with intensity  $I_L^v$  at the moment  $t$ , provided that its reorientation was given by  $\Omega_0$  at the moment  $t = 0$ , i.e.,

$$f(\Omega|\Omega_i, t, I_L^v) = \sum_{J,K,M,N} (2N+1) C_{KM}^{JN}(t, I_L^v) D_{KM}^{N*}(\Omega_0) D_{KM}^J(\Omega_i), \quad [2]$$

where  $D_{KM}^J, \dots$  are Wigner functions (14). The coefficients  $C_I(I_L^v)$  of the expansion of  $f(\Omega_0, I_L^v)$  in Wigner functions determine the stationary probability density distribution function in the external field  $\mathbf{E}_L$  of the strong laser beam. We have

$$f(\Omega_0, I_L^v) = \sum_I C_I(I_L^v) D_{00}^I(\Omega_0). \quad [3]$$

The functions  $C_I(I_L^v)$  can be expressed as linear combinations of Langevin–Kielich functions (see Refs. 8, 12, 19). The Langevin–Kielich functions  $L_n(\pm q_L^v)$  are defined as (12)

$$L_n(\pm q_L^v) = \frac{\int_0^\pi \cos^n \vartheta \exp(\pm q_L^v \cos^2 \vartheta) \sin \vartheta d\vartheta}{\int_0^\pi \exp(\pm q_L^v \cos^2 \vartheta) \sin \vartheta d\vartheta}, \quad [4]$$

where  $\vartheta$  is the angle between the symmetry axis  $s$  and the direction of the field  $\mathbf{E}_L$  of the strong laser beam of intensity  $I_L^v$  and frequency  $\omega_L$ , and

$$q_L^v(\omega_L) = \frac{a_3^{\omega_L} - a_1^{\omega_L}}{2k'T} I_L^v \quad [4a]$$

is the dimensionless reorientation parameter of the ellipsoid of optical polarizabilities at the laser frequency  $\omega_L$ . Moreover,  $k'$  is Boltzmann's constant and  $T$  is the temperature (in Kelvin).

The successive coefficients  $C_I(I_L^v)$  are of the form (12):

$$\begin{aligned} C_0 &= 1, \\ C_1 &= 3L_1(\pm q_L^v), \\ C_2 &= \frac{3}{2}[3L_2(\pm q_L^v) - 1], \\ C_3 &= \frac{7}{2}[5L_3(\pm q_L^v) - 3L_1(\pm q_L^v)]. \dots \end{aligned} \quad [5]$$

The analytical form of the dynamic coefficients  $C_{0M}^{JN}(t, I_L^v)$  is found by solving the Smoluchowski–Debye equation for spherical top molecules (10, 20) on the assumption that in a first approximation the molecular translational and rotational motions are statistically independent. If the field  $\mathbf{E}_L$  is directed along the  $Z$ -axis,  $C_{0M}^{JN}(t, I_L^v)$  involve only the rotational coefficient  $D_\perp$  of diffusion about the axis perpendicular to the symmetry axis of the macromolecule, whereas the rotational coefficient  $D_\parallel$  about the parallel axis are insignificant. Alexiewicz *et al.* (18) have solved the resulting Smoluchowski–Debye equation by the method of statistical perturbation calculus. They expanded the coefficients  $C_{0M}^{JN}(t, I_L^v)$  in a power series of  $\beta = 1/k'T$ , the reciprocal of the thermal motion energy. Here, we rewrite the expansion  $C_{0M}^{JN}(t, I_L^v)$  in a slightly different manner than originally written in (18),

$$C_{0M}^{JN}(t, I_L^v) = \sum_{s=0}^{\infty} \beta^s {}^{(s)} C_{0M}^{JN}(t, I_L^v), \quad [6]$$

where

$$\begin{aligned}
& {}^{(s)}C_{0M}^{JN}(t, I_L^v) \\
&= \frac{1}{6} \beta^{-1} q_L^v \sum_{J'=|J-2|}^{|J+2|} \frac{J(J+1) - J'(J'+1) + 6}{J(J+1)} \\
&\quad \times \begin{bmatrix} J' & 2 & J \\ 0 & 0 & 0 \end{bmatrix} \begin{bmatrix} J' & 2 & J \\ M & 0 & M \end{bmatrix} \frac{1}{\tau_J} \exp(-t/\tau_J) \\
&\quad \times \int_0^t \exp(t/\tau_J)^{(s-1)} C_{0M}^{J'N}(t, I_L^v) dt \quad [7]
\end{aligned}$$

For free rotational diffusion  $s = 0$  they found (18)

$${}^{(0)}C_{0M}^{JN}(t) = \frac{1}{8\pi^2} \delta_{JN} \exp(-t/\tau_J), \quad [8]$$

where the  $\tau_J$  are Debye rotational relaxation times, related as follows with the rotational diffusion coefficient  $D_{\perp}$ :

$$\tau_J = \frac{1}{J(J+1)D_{\perp}}. \quad [9]$$

With regard to Eq. [1] and the data of Table 1, in conformity with the experimental conditions adopted in Fig. 1, we finally arrive at the following expressions for the individual components of the time-autocorrelation function of light, scattered by solutions of rodlike and disclike macromolecules reoriented by the external electric field of a strong laser beam of intensity  $I_L^v$ :

$$\begin{aligned}
\frac{H_v^v(q', t)}{I_{zz}^0(t)} &= \frac{V_h^v(q', t)}{I_{xx}^0(t)} \\
&= A' \kappa_{\omega}^2 \exp(-q'^2 D_{\perp} t) \sum_n \sum_{n'} \sum_G \sum_I \sum_J \sum_M \sum_N i^n (-i)^{n'} \\
&\quad \times \frac{2N+1}{2I+1} \frac{\sqrt{2n'+1}}{\sqrt{2n+1}} C_I(I_L^v) C_{0M-1}^{JN}(t, I_L^v) Y_{nM}(\Omega_{q'}) \\
&\quad \times Y_{n',-M}(\Omega_{q'}) \begin{bmatrix} J & 2 & n \\ 0 & 0 & 0 \end{bmatrix} \begin{bmatrix} J & 2 & n \\ M-1 & 1 & M \end{bmatrix} \\
&\quad \times \begin{bmatrix} n' & 2 & G \\ 0 & 0 & 0 \end{bmatrix} \begin{bmatrix} n' & 2 & G \\ -M & 1 & 1-M \end{bmatrix} \begin{bmatrix} G & N & I \\ 0 & 0 & 0 \end{bmatrix} \\
&\quad \times \begin{bmatrix} G & N & I \\ 1-M & M-1 & 0 \end{bmatrix} b_n(x) b_{n'}(x), \quad [10]
\end{aligned}$$

$$\begin{aligned}
\frac{H_h^v(q', t)}{I_{xx}^0(t)} &= A' \kappa_{\omega}^2 \exp(-q'^2 D_{\perp} t) \sum_n \sum_{n'} \sum_G \sum_I \sum_J \sum_M \sum_N i^n (-i)^{n'} \\
&\quad \times \frac{2N+1}{2I+1} \frac{\sqrt{2n'+1}}{\sqrt{2n+1}} C_I(I_L^v) C_{0M-2}^{JN}(t, I_L^v) Y_{nM}(\Omega_{q'}) \\
&\quad \times \begin{bmatrix} J & 2 & n \\ 0 & 0 & 0 \end{bmatrix} \begin{bmatrix} J & 2 & n \\ M-2 & 2 & M \end{bmatrix} \begin{bmatrix} G & N & I \\ 0 & 0 & 0 \end{bmatrix} \\
&\quad \times \begin{bmatrix} G & N & I \\ 2-M & M-2 & 0 \end{bmatrix} \begin{bmatrix} n' & 2 & G \\ 0 & 0 & 0 \end{bmatrix} \\
&\quad \times \left\{ Y_{n',-M}(\Omega_{q'}) \begin{bmatrix} n' & 2 & G \\ -M & 2 & 2-M \end{bmatrix} + Y_{n',4-M}(\Omega_{q'}) \right. \\
&\quad \left. \times \begin{bmatrix} n' & 2 & G \\ 4-M & -2 & 2-M \end{bmatrix} \right\} b_n(x) b_{n'}(x), \quad [11]
\end{aligned}$$

$$\begin{aligned}
\frac{V_{zz}^v(q', t)}{I_{zz}^0(t)} &= \frac{1}{3} A' \exp(-q'^2 D_{\perp} t) \sum_{n'} \sum_I \sum_J \sum_M \sum_N (-i)^{n'} \\
&\quad \times \frac{2N+1}{2I+1} \frac{\sqrt{2n'+1}}{\sqrt{2n+1}} C_I(I_L^v) C_{0M}^{JN}(t, I_L^v) Y_{n',-M}(\Omega_{q'}) \\
&\quad \times \left\{ \frac{i'}{\sqrt{2J+1}} Y_{JM}(\Omega_{q'}) d_J(x) + 2\kappa_{\omega} \sum_n \frac{i^n}{\sqrt{2n+1}} Y_{nM}(\Omega_{q'}) \right. \\
&\quad \times \begin{bmatrix} J & 2 & n \\ 0 & 0 & 0 \end{bmatrix} \begin{bmatrix} J & 2 & n \\ M & 0 & M \end{bmatrix} b_n(x) \left. \right\} \\
&\quad \times \left\{ \sum_G \begin{bmatrix} n' & N & I \\ 0 & 0 & 0 \end{bmatrix} \begin{bmatrix} n' & N & I \\ -M & M & 0 \end{bmatrix} d_{n'}(x) \right. \\
&\quad \left. + 2\kappa_{\omega} \begin{bmatrix} n' & 2 & G \\ 0 & 0 & 0 \end{bmatrix} \begin{bmatrix} n' & 2 & G \\ M & 0 & M \end{bmatrix} \begin{bmatrix} G & N & I \\ 0 & 0 & 0 \end{bmatrix} \right. \\
&\quad \left. \times \begin{bmatrix} G & N & I \\ -M & M & 0 \end{bmatrix} b_{n'}(x) \right\}, \quad [12]
\end{aligned}$$

where, for example,  $H_v^v$  [12] denotes the horizontal component of the scattered light intensity (capital letter  $H$ ) at vertical polarization of the incident probe light (subscript  $v$ ) and vertical polarization of the reorienting external laser field (superscript  $v$ ). The symbols  $H_h^v$ ,  $V_h^v$ , and  $V_v^v$  are interpreted analogously. For details see Fig. 1.

### 3. DISCUSSION

With the form of the time-autocorrelation function  $I_{ij}^v(q', t)$  (Eq. [1]) available, we are able to derive the expression for the spectral density  $I_{ij}^v(q', \Delta\omega)$  of the scattered

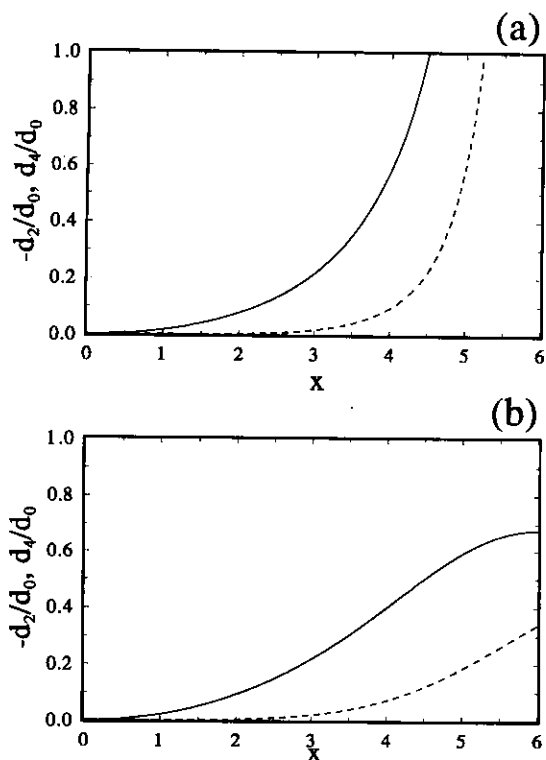


FIG. 2. The ratios  $-d_2/d_0$  (solid lines) and  $d_4/d_0$  (dashed lines) versus the parameter  $x$  for (a) discs,  $x = q'a_D$ , and (b) rods,  $x = q'l/2$ .

light intensity tensor by applying the Wigner-Khintchine relation (21)

$$I_{ij}^v(q', \Delta\omega) = \mathcal{F}_t I_{ij}^v(q', t), \quad [13]$$

where  $\mathcal{F}_t$  is the Fourier transform. We shall now discuss the influence of the size and shape of the macromolecules as well as the influence of the reorientation parameter  $q_L^v \equiv q_L^v(\omega_L)$  on the spectral lineshapes of the individual components (Eqs. [10]–[12]) of light scattered by solutions of rodlike and disclike macromolecules at a low degree of reorientation in the external electric field of a laser beam of intensity  $I_L^v$ . In the present case, the dynamic coefficients  $C_{0M}^{JN}(t, I_L^v)$  (Eq. [6]) can be expressed in the form of the approximation

$$C_{0M}^{JN}(t, I_L^v) = {}^{(0)}C_{0M}^{JN}(t, I_L^v) + {}^{(1)}C_{0M}^{JN}(t, I_L^v), \quad [14]$$

where the successive terms are calculated with Eqs. [7] and [8]. The expansion coefficients  $C_I(I_L^v)$  (Eq. [5]) are nonzero for subscripts  $I = 0, 2$  only. To determine the respective relations for  $C_I(I_L^v)$ , we must expand the Langevin-Kielich functions (Eq. [4]) in series in  $q_L^v$  leading to (8, 12):

$$\begin{aligned} C_0 &= 1, \\ C_1 &= 0, \\ C_2 &= \frac{2}{3}q_L^v. \end{aligned} \quad [15]$$

In accordance with the assumptions made, the angular coordinates of  $\mathbf{q}'$  are (Fig. 1)

$$\mathbf{q}' = 2k \sin \frac{\theta}{2} \left[ \hat{\mathbf{x}} \sin \frac{\theta}{2} - \hat{\mathbf{y}} \cos \frac{\theta}{2} \right], \quad [16]$$

hence

$$\Omega_{q'} = \left( \frac{\pi}{2}, \frac{\theta}{2} - \frac{\pi}{2} \right), \quad [17]$$

where  $q' = 2k \sin(\theta/2)$  ( $\theta = \pi/2$  is the angle at which we chose to observe the experiment of light scattering). The shape functions  $d_n(x)$  and  $b_n(x)$  (Eqs. [1a] and [1b]) are taken for  $n = 0, 2$  only. Terms for higher-order approximations ( $n = 4, 6, \dots$ ) take much smaller values (see Fig. 2) compared to  $n = 0, 2$ , so we omit them. We obtain from the definitions [1a] and [1b] the following expressions: (i) for rodlike macromolecules

$$\begin{aligned} d_0^R(x) &= \frac{\text{Si}(x)}{x}, \\ d_2^R(x) &= \frac{-3 \sin x}{2x^3} + \frac{3 \cos x}{2x^2} + \frac{\text{Si}(x)}{2x}, \end{aligned} \quad [18]$$

and (ii) for disclike macromolecules

$$\begin{aligned} d_0^D(x) &= \frac{2}{x^2} (1 - \cos x), \\ d_2^D(x) &= -\frac{1}{x^2} (\cos x + 2) + \frac{3}{x^3} \sin x, \end{aligned} \quad [19]$$

where, at  $\theta = \pi/2$ , we have  $x = \sqrt{2}\pi l/\lambda$  for rods and  $x = 2\sqrt{2}\pi a_D/\lambda$  for discs;  $\text{Si}(x)$  is the integral sine function. In the limit  $x \rightarrow 0$ , the shape functions [18] and [19] tend to

$$\begin{aligned} \lim_{x \rightarrow 0} d_0(x) &= 1, \\ \lim_{x \rightarrow 0} d_2(x) &= 0. \end{aligned} \quad [20]$$

With regard to the preceding relations, one can express as follows the Fourier transforms of the components  $H_{ij}^v(q', t)$ ,  $H_h^v(q', t)$ , and  $V_{ij}^v(q', t)$  for a low degree of orientation of macromolecules in an external laser field and

on approximating  $d_n \equiv d_n(x)$  and  $b_n \equiv b_n(x)$  to the order  $n = 2$ :

$$\begin{aligned} \frac{H_v^y(\Delta\omega)}{I_{zz}^0} &= A''\kappa_\omega^2 \left\{ L_2(\Delta\omega) \left( \frac{b_0^2}{20} + \frac{b_0b_2}{28} + \frac{25b_2^2}{392} \right) \right. \\ &+ L_4(\Delta\omega) \frac{45b_2^2}{392} + q_L^y \left[ L_2(\Delta\omega) \left( \frac{b_0^2}{210} + \frac{37b_0b_2}{2058} + \frac{25b_2^2}{7203} \right) \right. \\ &+ L_4(\Delta\omega) \left( \frac{2b_0b_2}{343} + \frac{205b_2^2}{105,644} \right) + G_2(\Delta\omega) \\ &\left. \left. \times \left( \frac{b_0^2}{420} + \frac{b_0b_2}{588} + \frac{25b_2^2}{8232} \right) + G_4(\Delta\omega) \frac{27b_2^2}{60,368} \right] \right\}, \quad [21] \end{aligned}$$

$$\begin{aligned} \frac{H_h^x(\Delta\omega)}{I_{xx}^0} &= A''\kappa_\omega^2 \left\{ L_2(\Delta\omega) \left( \frac{b_0^2}{20} - \frac{b_0b_2}{14} + \frac{5b_2^2}{196} \right) \right. \\ &+ L_4(\Delta\omega) \frac{15b_2^2}{98} - q_L^x \left[ L_2(\Delta\omega) \left( \frac{b_0^2}{105} - \frac{43b_0b_2}{2058} \right. \right. \\ &+ \left. \left. \frac{145b_2^2}{14,406} \right) - L_4(\Delta\omega) \left( \frac{b_0b_2}{343} - \frac{1755b_2^2}{52,822} \right) + G_2(\Delta\omega) \right. \\ &\left. \left. \times \left( \frac{b_0^2}{210} - \frac{b_0b_2}{147} + \frac{5b_2^2}{2058} \right) + G_4(\Delta\omega) \frac{141b_2^2}{30,184} \right] \right\}, \quad [22] \end{aligned}$$

$$\begin{aligned} \frac{V_z^y(\Delta\omega)}{I_{zz}^0} &= A'' \left\{ L_T(\Delta\omega) \left( \frac{\kappa_\omega^2 b_2^2}{12} + \frac{\kappa_\omega b_2 d_0}{6} + \frac{d_0^2}{12} \right) \right. \\ &+ L_2(\Delta\omega) \left( \frac{\kappa_\omega^2 b_0^2}{15} + \frac{2\kappa_\omega^2 b_0 b_2}{21} + \frac{20\kappa_\omega^2 b_2^2}{147} + \frac{\kappa_\omega b_0 d_2}{6} \right. \\ &- \left. \frac{5\kappa_\omega b_2 d_2}{21} + \frac{5d_2^2}{12} \right) + L_4(\Delta\omega) \frac{27\kappa_\omega^2 b_2^2}{196} + q_L^y \left[ L_T(\Delta\omega) \right. \\ &\times \left( \frac{2\kappa_\omega^2 b_0 b_2}{45} + \frac{2\kappa_\omega^2 b_2^2}{63} + \frac{2\kappa_\omega b_0 d_0}{45} + \frac{2\kappa_\omega b_2 d_0}{63} + \frac{\kappa_\omega b_2 d_2}{18} \right. \\ &+ \left. \frac{d_0 d_2}{18} \right) + L_2(\Delta\omega) \left( \frac{4\kappa_\omega^2 b_0^2}{315} + \frac{128\kappa_\omega^2 b_0 b_2}{3087} - \frac{370\kappa_\omega^2 b_2^2}{21,609} \right. \\ &+ \left. \frac{2\kappa_\omega b_0 d_2}{63} + \frac{965\kappa_\omega b_2 d_2}{6174} - \frac{5d_2^2}{126} \right) + L_4(\Delta\omega) \\ &\left. \left. \times \left( \frac{16\kappa_\omega^2 b_0 b_2}{1715} + \frac{376\kappa_\omega^2 b_2^2}{26,411} + \frac{9\kappa_\omega b_2 d_2}{343} \right) + G_2(\Delta\omega) \right] \right\} \end{aligned}$$

$$\begin{aligned} &\times \left( \frac{2\kappa_\omega^2 b_0^2}{315} + \frac{4\kappa_\omega^2 b_0 b_2}{441} - \frac{20\kappa_\omega^2 b_2^2}{3087} + \frac{\kappa_\omega b_0 d_2}{63} \right. \\ &\left. + \frac{20\kappa_\omega b_2 d_2}{441} - \frac{5d_2^2}{252} \right) + G_4(\Delta\omega) \frac{9\kappa_\omega^2 b_2^2}{3773} \left. \right\}, \quad [23] \end{aligned}$$

and the function  $A''$  is equal to  $A'/8\pi^3$ . The functions  $L_J(\Delta\omega)$  occurring in Eqs. [21]–[23] are Lorentzians determining the Lorentz shape of the scattered light spectrum, with

$$L_J(\Delta\omega) = \frac{1}{\pi} \frac{\tau_J(1 + (\tau_J/\tau_T))}{(1 + (\tau_J/\tau_T))^2 + (\Delta\omega\tau_J)^2}, \quad [24a]$$

$$L_T(\Delta\omega) \equiv L_0(\Delta\omega) = \frac{1}{\pi} \frac{\tau_T}{1 + (\Delta\omega\tau_T)^2}, \quad [24b]$$

whereas the functions  $G_J(\Delta\omega)$ , given by

$$G_J(\Delta\omega) = \frac{\tau_J}{\pi} \frac{(1 + (\tau_J/\tau_T))^2 - (\Delta\omega\tau_J)^2}{[(1 + (\tau_J/\tau_T))^2 + (\Delta\omega\tau_J)^2]^2}, \quad [25]$$

are the non-Lorentzian contributions to the spectral line-shape. The translational relaxation time  $\tau_T$  of the macromolecule is given by

$$\tau_T = \frac{1}{q'^2 D_T}. \quad [26]$$

The function  $G_J(\Delta\omega)$  (Eq. [25]) never occurs independently. It intervenes only as an additional component of the superposition of Lorentzian factors (Eq. [24]). In the limit, when  $\tau_J \gg \tau_T$  ( $J > 0$ ), the Lorentzian (Eq. [24]) and non-Lorentzian (Eq. [25]) functions simplify considerably, describing only the rotational diffusion of the macromolecules. The results are presented elsewhere (8). Here, we analyze various macromolecular components with the rotational and translational relaxation times of the same order. In case of predominant translational diffusion of the macromolecules, i.e., for  $\tau_J \ll \tau_T$ , the functions [24] and [25] tend to be independent of  $\Delta\omega$  with increasing  $\tau_J$ .

In the special case when  $x < 1$  (see Fig. 3), our formulas [21]–[23] simplify considerably, leading to the expressions

$$\begin{aligned} \frac{H_v^y(\Delta\omega)}{I_{zz}^0} &= \frac{1}{20} A'' \kappa_\omega^2 [L_2(\Delta\omega) + \frac{1}{21} q_L^y (2L_2(\Delta\omega) \\ &+ G_2(\Delta\omega))] b_0^2(x), \quad [27] \end{aligned}$$

$$\begin{aligned} \frac{H_h^x(\Delta\omega)}{I_{xx}^0} &= \frac{1}{20} A'' \kappa_\omega^2 [L_2(\Delta\omega) - \frac{2}{21} q_L^x (2L_2(\Delta\omega) \\ &+ G_2(\Delta\omega))] b_0^2(x), \quad [28] \end{aligned}$$

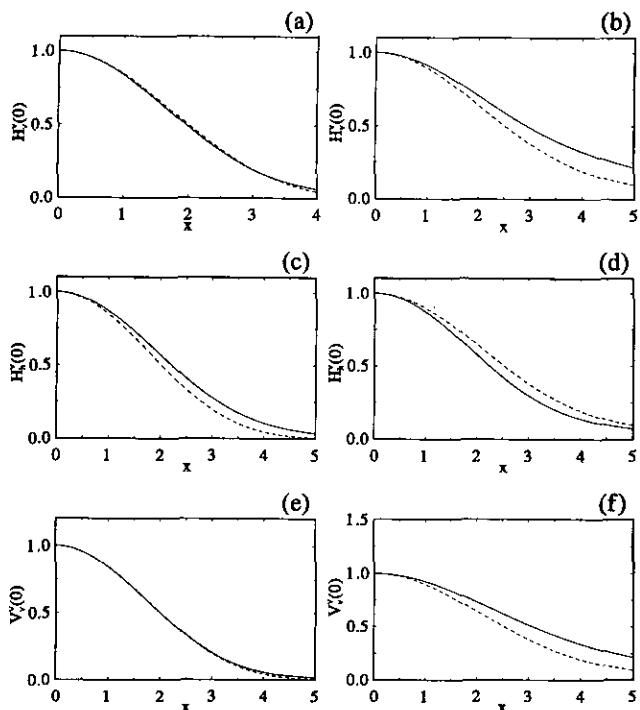


FIG. 3. The maximum (for  $\Delta\omega = 0$ ) of the spectral lineshapes of the normalized scattered light components  $H_v^v(0) \equiv H_v^v(\Delta\omega = 0)$  (a, b),  $H_h^h(0)$  (c, d), and  $V_v^v(0)$  (e, f) versus the parameter  $x$  for discs (a, c, e) at  $q_L^v = -0.5$ ,  $\kappa = -0.4$  and rods (b, d, f) at  $q_L^v = 0.5$ ,  $\kappa = 0.4$ . Solid lines are depicted according to Eqs. [21]–[23], whereas dashed lines are given according to Eqs. [27]–[29]. The normalization is chosen to fulfill the conditions:  $H_v^v(\Delta\omega = 0, a_D/\lambda = l/\lambda = 0) = H_h^h(0, a_D/\lambda = l/\lambda = 0) = V_v^v(0, a_D/\lambda = l/\lambda = 0) = 1$ .

$$\frac{V_v^v(\Delta\omega)}{I_{zz}^0} = \frac{1}{15}A'' \{ \kappa_\omega^2 [L_2(\Delta\omega) + \frac{2}{21}q_L^v(2L_2(\Delta\omega) + G_2(\Delta\omega))] b_0^2(x) + \frac{2}{3}\kappa_\omega q_L^v L_T(\Delta\omega) b_0(x) d_0(x) + \frac{5}{3}L_T(\Delta\omega) d_0^2(x) \}, \quad [29]$$

which go over into Lorentzians for  $q_L^v = 0$ .

From Fig. 2, the order  $n$  of the shape functions [1a] and [1b] considered by us, namely  $n = 0, 2$ , restricts the range of  $x$  values for which the formulas [21]–[23] hold. It is seen from this figure that higher-order shape functions should be taken into account for  $x > 4$ , particularly for disclike molecules.

Thus, the formulas obtained by us for the components [21]–[23] at low macromolecular reorientation in the external laser field and their numerical analysis (Figs. 3–5) hold for rodlike macromolecules with dimensions  $l < \lambda$  and for disclike ones with  $a < 0.5\lambda$ .

Figure 3 shows the  $x$ -dependence of the components  $H_v^v(\Delta\omega = 0)$ ,  $H_h^h(\Delta\omega = 0)$ , and  $V_v^v(\Delta\omega = 0)$ , calculated from Eqs. [21]–[23] (solid lines) and approximate relations

[27]–[29] (dashed lines). It is seen that the smallest contribution of the shape functions  $d_2(x)$  is for the values of  $H_v^v(0)$  and  $V_v^v(0)$  in case of disclike molecules. Hence, one can use our approximate expressions [27] and [29] for these components throughout the depicted range of  $x$ . The line intensities of the components [21]–[23] decrease markedly for large macromolecules compared with the intensities observed for small macromolecules ( $l \ll \lambda$ ,  $a_D \ll \lambda$ ) as presented in Fig. 4. The greater the values of  $l/\lambda$  and  $a_D/\lambda$ , the weaker are the intensities, particularly for disclike macromolecules.

In Fig. 5 we have depicted the components [21]–[23] for various values of the reorientation parameter  $q_L^v$ . The differences between the respective components for different  $q_L^v$  become more pronounced with decreasing values of  $l/\lambda$  ( $a_D/\lambda$ ) and increasing  $x$ . The components  $H_v^v(\Delta\omega)$  (Figs. 5a and 5b) and  $V_v^v(\Delta\omega)$  (Figs. 5e and 5f) at nonzero  $q_L^v$  are greater than those at  $q_L^v = 0$  for rods but smaller for discs. In the case of the component  $H_h^h(\Delta\omega)$  (Figs. 5c and 5d) the line intensity at  $q_L^v \neq 0$  is lower than that at  $q_L^v = 0$  for rods and higher for discs. Thus, the line intensity measured at  $\Delta\omega = 0$  allows the determination of the size and sign of the anisotropy of the macromolecules. Similar conclusions have been reached by Alexiewicz *et al.* (18) in their studies of small macromolecules. Also, results obtained in (30, 31)

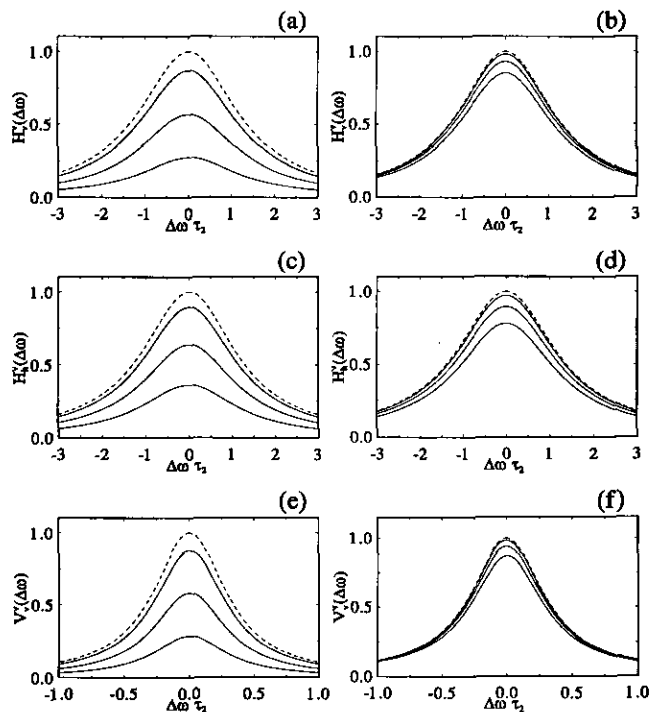


FIG. 4. The spectral lineshapes of the normalized scattered light components  $H_v^v(\Delta\omega)$  (a, b),  $H_h^h(\Delta\omega)$  (c, d), and  $V_v^v(\Delta\omega)$  (e, f) for discs (a, c, e) at  $q_L^v = -0.5$ ,  $\kappa = -0.4$  and rods (b, d, f) at  $q_L^v = 0.5$ ,  $\kappa = 0.4$  for different values of the ratio  $a_D/\lambda = l/\lambda = 0$  (dashed line), and 0.1, 0.2, 0.3 (solid lines) with the same normalization as for Fig. 3.

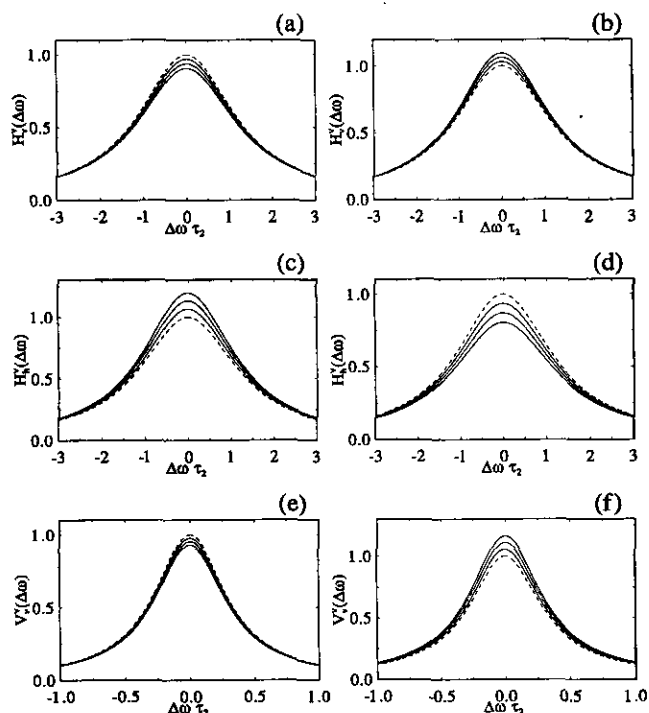


FIG. 5. The spectral lineshapes of the normalized scattered light components  $H_v^v(\Delta\omega)$  (a, b),  $H_h^v(\Delta\omega)$  (c, d), and  $V_v^v(\Delta\omega)$  (e, f) for discs (a, c, e) at  $q_L^z = 0$  (dashed lines),  $-0.25$ ,  $-0.5$ ,  $-0.75$  (solid lines) and  $\kappa = -0.4$  as well as rods (b, d, f) at  $q_L^z = 0$  (dashed lines),  $0.25$ ,  $0.5$ ,  $0.75$  (solid lines), and  $\kappa = 0.4$  for the ratio  $a_D/\lambda = l/\lambda = 0.1$ . The normalization is:  $H_v^v(\Delta\omega = 0, q_L^z = 0) = H_h^v(\Delta\omega = 0, q_L^z = 0) = V_v^v(\Delta\omega = 0, q_L^z = 0) = 1$ .

for integral components of light scattering are in agreement with those presented here.

Here, we have not considered the effect of a laser field on the translational motion of the macromolecules. However, at high anisotropy of the translational diffusion coefficients  $(D_{\parallel}^T - D_{\perp}^T)/D^T$ , the statistical distribution function contains terms which interrelate the translational and reorientational motions, so that the two processes of diffusion cannot be dealt with as statistically independent (22–26). As a consequence, in Eq. [1] for the heterodyne autocorrelation function, one has to take into consideration the translational effect due to the laser field (27–29). As an example of macromolecules for which the influence of the mutual interdependence between the translational and reorientational motions on the spectrum is very apparent, one should mention the case of the tobacco mosaic virus TMV, for which  $(D_{\parallel}^T - D_{\perp}^T)/D^T = 0.4$  (23).

## ACKNOWLEDGMENT

This work was carried out within the framework of Project PB 201309101 of the State Committee for Scientific Research.

## REFERENCES

1. Fabelinski, I. L., "Molecular Scattering of Light." Plenum, New York, 1968.
2. Berne, B. I., and Pecora, R., "Dynamic Light Scattering with Applications to Chemistry, Biology and Physics," Wiley-Interscience, New York, 1976.
3. Chu, B., "Laser Light Scattering." Academic Press, New York, 1974.
4. Kielich, S., *Proc. Indian Acad. Sci. Chem. Sci.* **94**, 403 (1985).
5. Kasprowicz-Kielich, B., Kielich, S., and Lalanne, J. R., in "Molecular Motions in Liquids" (L. Lascombe, Ed.), p. 563. Reidel, Dordrecht, 1974.
6. Alexiewicz, W., Buchert, J., and Kielich, S., *Acta Phys. Pol. A* **52**, 442 (1977).
7. Kielich, S., "Nonlinear Molecular Optics." Nauka, Moscow, 1981.
8. Dębska-Kotłowska, M., and Miranowicz, A., in "Modern Nonlinear Optics" (M. Evans and S. Kielich, Eds.), Prigogine and Rice Ser., Vol. 85, Part 1, p. 51. Wiley, New York, 1993.
9. Van de Hulst, H. C., "Light Scattering by Small Particles." Wiley, New York, 1957.
10. Debye, P., "Polare Molekeln." Hirzel, Leipzig, 1929.
11. Perrin, F., *J. Phys. Radium* **5**, 497 (1934).
12. Kielich, S., *Acta Phys. Pol. A* **37**, 447, 719 (1970).
13. Kielich, S., *Proc. Indian Acad. Sci. Chem. Sci.* **94**, 403 (1985).
14. Varshalovich, D. A., Moskalyev, A. N., and Khersonskii, V. K., "Quantum Theory of Angular Momentum." Nauka, Leningrad, 1975.
15. Ożgo, Z., "Multi-harmonic Molecular Light Scattering in the Treatment of Racach Algebra." UAM, Poznań, 1975.
16. Kielich, S., *Prog. Opt.* **20**, 155 (1983).
17. Aragon, S. R., and Pecora, R., *J. Chem. Phys.* **66**, 2506 (1977).
18. Alexiewicz, W., Buchert, J., and Kielich, S., *Phys. Dielectr. Radiospectr.* **9**, 5 (1977).
19. Evans, M. W., Woźniak, S., and Wagnière, G., *Physica B* **175**, 412 (1991).
20. "The Works of Marian Smoluchowski," Vol. 1 and 2, Jagellonian U. P., Cracow 1924 and 1927.
21. Wang, M. C., and Uhlenbeck, G. E., *Rev. Mod. Phys.* **17**, 323 (1945).
22. Maeda, H., and Saito, N., *Polymer J.* **4**, 309 (1973).
23. Maeda, H., and Saito, N., *J. Phys. Soc. Jpn.* **27**, 989 (1969).
24. Hwang, I. S., and Cummins, H. Z., *J. Chem. Phys.* **77**, 616 (1982).
25. Evans, M. W., *J. Chem. Phys.* **78**, 5403 (1983); **77**, 4632 (1982).
26. Evans, M. W., *Phys. Rev. A* **30**, 2062 (1984).
27. Storonkin, V. A., *L. G. Y. Vestnik*, No. 4. 1983.
28. Burghardt, T. P., *J. Chem. Phys.* **78**, 5913 (1983).
29. Tian, D., and McClain, W. M., *J. Chem. Phys.* **91**, 4435 (1989); **90**, 4783, 6956 (1989).
30. Horn, P., Thesis, Strasbourg, 1954.
31. Dębska-Kotłowska, M., and Kielich, S., *J. Polym. Sci. Polym. Symp.* **61**, 101 (1977).